water

MDPI

Article

Research on Extension Evaluation Method of Mudslide Hazard Based on Analytic Hierarchy Process–Criteria Importance through Intercriteria Correlation Combination Assignment of Game Theory Ideas

Hui Li [1,2], Xueshan Bai [1,2], Xing Zhai [1,2,*], Jianqing Zhao [1,2], Xiaolong Zhu [1,2], Chenxi Li [1,2], Kehui Liu [1] and Qizhi Wang [3]

[1] Hebei Geo-Environment Monitoring Institute, Shijiazhuang 050000, China; lihui2088@163.com (H.L.)
[2] Hebei Key Laboratory of Geological Resources and Environment Monitoring and Protection, Shijiazhuang 050000, China
[3] School of Civil Engineering, Hebei University of Science and Technology, Shijiazhuang 050000, China
* Correspondence: zhaib8188@163.com

Abstract: Mountain mudslides have emerged as one of the main geological dangers in the Yanshan region of China as a result of excessive rains. In light of this, a multi-step debris flow hazard assessment method combining optimal weights and a topological object metamodel is proposed based on game theory ideas. First of all, based on the geological environment research in Yanshan area, this paper determines the mudslide danger evaluation indexes according to the field investigation and remote sensing image data, then combines them with the theory of topological object element evaluation, utilizes the idea of game theory, and carries out the optimal combination of the weight coefficients derived from hierarchical analysis and the CRITIC method to obtain the final comprehensive weights of the indexes, and forms the combination-assigning topological object element of the mudslide danger topological model. The results suggest that improved weight coefficients can increase topological evaluation precision, which is more in line with objective reality than the traditional method and has some application utility.

Keywords: debris flow; topological theory; game theory ideas; analytic hierarchy process; CRITIC empowerment method; dangerousness

Citation: Li, H.; Bai, X.; Zhai, X.; Zhao, J.; Zhu, X.; Li, C.; Liu, K.; Wang, Q. Research on Extension Evaluation Method of Mudslide Hazard Based on Analytic Hierarchy Process–Criteria Importance through Intercriteria Correlation Combination Assignment of Game Theory Ideas. *Water* **2023**, *15*, 2961. https://doi.org/10.3390/w15162961

Academic Editor: Chin H Wu

Received: 3 July 2023
Revised: 13 August 2023
Accepted: 14 August 2023
Published: 17 August 2023

1. Introduction

China has the best mudslide study base, and many characteristic mudslides are unique [1], such as the Jiangjiagou debris flow, known as the "Natural Museum of Debris Flow"; the high-density viscous debris flow in Lizi Yidagou, Sichuan Province; and the extremely large debris flow in Zhouqu, Gansu Province. Debris flows have a short occurrence period, a large impact range, a high casualty rate, and a long recovery time as a geological disaster with sudden and random characteristics of combined water and rock movements [2–6]. Debris flows are caused by geological and environmental circumstances, rainfall, earthquakes, and other disaster-causing causes, as well as human engineering operations, and the method of development is complex and difficult to prevent and regulate; examples include catastrophic debris flows that happened in 2010 in the town of Qingping as a result of a strong earthquake and subsequent rainstorms working together [7], debris flows brought on by a glacial lake outburst flood in western Norway [8], and debris flows in pyroclastic deposits as a result of rainfall in Campania, Southern Italy [9].

Hebei Province, which has the most comprehensive geomorphological units in China, has active geological processes, intricate micro-geomorphological units, notable climatic differences, and severe weathering of geotechnical bodies, all of which contribute to the development of debris flows [10]. The Yanshan and Taihang Mountains in northern Hebei

are the main locations for debris flow development. Debris flows have become one of the main geological hazards that have developed in the area as a result of the rapid development of the national economy, the gradual expansion of human engineering activities, and the frequent occurrence of extreme rainfall, seriously endangering the lives and property of the populace.

Debris flows are caused by the interaction of natural and human forces, such as rainfall or earthquakes, in a specific geological setting. The study of debris flow hazard evaluation is built on investigation and mechanism research; debris flow investigation identifies the risk assessment influence factors, and motion evolution research identifies the contribution of each influence factor to the formation and evolution of debris flows. Since the last century, a significant deal of work has been performed, major accomplishments have been made, and new technology and methods have raised the caliber of kinematic evolution research and debris flow study. Vagnon Federico, Kiefer Carolin, and others carried out geomorphological examinations of debris flows and fans using modern technologies, including geophysical and geomorphological surveys. In terms of debris flow investigation, Vagnon Federico and Kiefer Carolin have used new technologies such as geophysical and geomorphological surveys to carry out geomorphological investigations of debris flows and fan areas, construct numerical models, and reveal the evolution of debris flow formation [11–14]; the Delphi technique was utilized by Byun Yo Seph et al. for debris flows that did not fit the criteria for a normal study and organized 12 experts to carry out a debris flow survey for preliminary assessment [15]. Bezak Nejc et al. investigated potential debris flows above the Koroška Bela settlement, NW Slovenia, from the hydro-technical and conceptual design perspectives [16]; Peng B. et al. introduced digital twin technology to high-precision geological hazard survey and prevention and carried out an analysis of geohazard development characteristics to study their hazards [17]. In the study of debris flow motion evolution, a new understanding of fluid–particle coupling evolution was obtained by simulating several debris flows' hydrological processes through indoor experiments [18–20]; a great deal of work was performed on the analysis of debris flow rheological evolution by unmanned aerial photography and radar technology to provide a basis for risk assessment [21,22].

Debris flow hazard is the probability of occurrence in a specific location over time due to the action of predisposing factors, and the evaluation methods and results are important in debris flow prediction and prevention [23,24]. Eldeen established the hazard level by drawing a debris flow hazard map [25]; Hollingsworth et al. created a framework for evaluating debris flow hazards, chose three evaluation factors, and established five classes to do so [26]; and Ohmori H et al. used the debris flow occurrence scale and outbreak frequency as evaluation factors in debris flow hazard evaluation [27]. In the 1990s, the application of GIS and RS technologies provided strong support for debris flow hazard evaluation. Carrara A. et al. used geographic information technology in landslide debris flow risk evaluation [28–30]; Raimon Pallàs et al. conducted debris flow hazard assessment based on the GIS system platform [31–33]; and Christopher Gomez et al. used 3D point cloud technology and airborne laser technology from aerial photogrammetry for debris flow hazard assessment [34]. Computer technology offers a more straightforward and accurate computational tool for debris flow evaluation, and numerical simulation is frequently employed in the assessment of debris flow hazard [35–39]; the integration of debris flow hazard evaluation algorithms and computers provides new ideas and methods for hazard evaluation [40–43]; Nie Yinping et al. used the optimized Flow-R coupled model for debris flow hazard assessment and achieved better evaluation results [44,45]; and artificial intelligence was also gradually applied in debris flow hazard evaluation, and the evaluation model was constructed by training and learning from a large number of sample sets to improve the evaluation accuracy [46,47]. Li Qianqian et al. used physical model experiments to conduct debris flow hazard evaluation to better understand the debris flow formation mechanism and estimate the debris flow danger zone [48,49].

In conclusion, it has been discovered that evaluation indexes are the crucial foundation of danger assessment in debris flow hazard evaluation, and the choice of reasonable evaluation indexes following a thorough investigation into debris flows is conducive to improving the evaluation's quality. As a result, further discussion regarding the development of a set of evaluation criteria and an evaluation level of work in line with the local reality is required. Secondly, the weight coefficient is crucial to the evaluation process, and a single weight calculation method is frequently based on subjective or objective methods, making it challenging to take into account the expert's understanding of the evaluation index, its volatility and relevance, and the efficient combination of two weight coefficients using a reasonable combination of assignment methods; further research is required on the combining of evaluation index systems to create a set of evaluation systems and a set of practicable evaluation procedures. Therefore, this study combines the findings of previous studies, accounting for the indicators of debris flow development characteristics, introducing evaluation indicators like the melton ratio and basin elongation, using phase relationship analysis to determine the evaluation index level, computing the evaluation index weight coefficients from subjective and objective aspects, respectively, using the hierarchical analysis process and the CRITIC method, and applying game theory for combination assignment to determine the combination weight coefficients; based on this, the extension theory is used to introduce the correlation function to form the evaluation system and determine the evaluation level of debris flow hazard, which provides the theoretical basis for debris flow prevention and control. Through comparative verification, the optimized weight-based topological evaluation method eliminates subjective and objective adverse effects on the evaluation and is more practical than other methods, such as the recognition of qualitative and related technical requirements in the wild and the evaluation of the information quantity method.

2. Study Area

2.1. Overview of the Evaluation Area

The evaluation location is in the Yanshan mountainous area of east Hebei, and the mudslides are more developed, being generally typical rainfall-type mudslides that are influenced by natural processes. With regard to meteorological aspects, the study area's climate is the temperate continental monsoon-type Yanshan mountain climate, the inter-annual and intra-annual distribution of precipitation is uneven, and summer rainfall from July to September accounted for 65–75% of total annual precipitation, mostly in the form of concentrated rainfall and heavy rainfall. In terms of topography and geomorphology, the terrain of the study area is high in the northwest and low in the southeast, with hills dominating the landscape; the Yanshan Mountains have formed a significant number of small intermountain basins and wide valleys due to tectonics, erosion, and accretion. These basins are distributed in the form of a series of beads, and small intermountain valley basins are frequently formed at the intersection of gullies and valleys. In terms of tectonics, the study area is characterized by the development of rupture and fold tectonics, which has gone through the three major phases of basement formation, cover development, and intense activity, spanning two geotectonic units: the relatively active Inner Mongolia–Daxinganling fold system in the north, and the relatively stable North China Plateau in the south. In terms of lithology, the stratigraphy is relatively complete, the bedrock is widely distributed, and the lithology is dominated by gneiss, dolomite, limestone, sandstone, and gravel; human engineering activities are more intense (Figure 1).

Figure 1. Photographs of the topography and geomorphology of the study area.

2.2. Determination of Debris Flow Hazard Evaluation Index

By examining the development characteristics and distribution pattern of debris flows in Jidong Yanshan's mountainous regions, we were able to categorize the 310 debris flows' development characteristics and influencing factors, such as topography and geomorphology, stratigraphic lithology, geological structure, and rainfall, and determine evaluation indices such as the melton ratio, vegetation NDVI index, basin elongation, loose material reserves, and height difference rate, slope, average annual precipitation, and distance from structure [50–52]. Melton ratio, basin elongation, height difference rate, and hillside slope are a few indices that show the topographic changes in the mudslide watershed at various angles and are significant indicators of the scouring and erosion of the material sources, gully, and ravine slopes by surface water runoff; vegetation NDVI index reflects the stability of the material sources of mudslides, which is an evaluation indicator of the degree of susceptibility to the mudslides; the loose material reserve capacity and the distance from the structure are the material conditions, which are indicators of the number of material sources when mudslides occur; average annual rainfall reflects the conditions of mudslide triggering, which are the driving conditions of mudslides.

(1) melton ratio (c_1).

The melton ratio, a crucial predictor of the transport of debris flow material sources, represents topography variation within the debris flow basin. The higher the melton ratio, the steeper and straighter the terrain of the debris flow basin, the more kinetic energy available for the source loose material, and hence, the greater the risk; conversely, the lower the kinetic energy, the lower the risk.

$$R_m = H/\sqrt{A} \tag{1}$$

where H is the height difference of the debris flow basin, and A is the area of the debris flow basin.

(2) Vegetation NDVI index (c_2).

The vegetation NDVI index reflects the degree of debris flow vegetation cover, which is also an important indicator of the stability of debris flow material sources. The stronger the NDVI index, the better the vegetation cover, the more conducive to the stability of debris flow sources, and the lower the risk; conversely, the less vegetation cover, the larger the risk is.

(3) Basin elongation (c_3).

Basin elongation responds to changes in the shape of the debris flow basin and is an indicator of the impact of debris flow catchment velocity and flow intensity. The closer the indicator is near 1, the more similar the debris flow basin form is to a circle, and vice versa for a narrow strip. When the basin is circular, the tributaries can converge and reach the

outflow more quickly, the peak flow at the outlet is higher than it would be in a narrow ribbon basin, and the risk of debris flows is higher.

$$EI = \frac{2\sqrt{A}}{L\sqrt{\pi}} \tag{2}$$

where L is the maximum length of the debris flow basin.

(4) Loose material reserves capacity (c_4).

The amount of loose material reserves is one of the three elements of debris flow occurrence. The larger the storage, the greater the risk of debris flow; conversely, the smaller the storage, the smaller the risk.

(5) Height difference rate (c_5).

The height difference rate reflects the slope drop of the debris flow, which is an indicator of the flow velocity and kinetic energy of the debris flow. The higher the height difference rate, the greater the debris flow hazard; conversely, the lower the height difference, the smaller the hazard.

$$R_r = H/L \tag{3}$$

(6) Hillside slope (c_6).

The hillside slope is the slope on both sides of the debris flow gully. The larger the slope, the more unstable the slope, the greater the surface water pooling energy, and thus, the greater the risk of debris flows; conversely, the smaller the slope, the lower the risk.

(7) Average annual precipitation (c_7).

The average annual precipitation provides energy for the occurrence of debris flows and is the primary predisposing factor in the study area. The greater the rainfall, the greater the risk of debris flow; conversely, the smaller the rainfall, the lower the risk.

(8) Distance from structure (c_8).

The distance from the structure is the distance from the debris flow to the fault zone. The closer the debris flow is to the fracture zone, the more fragmented the rock and soil body in the watershed is, the higher the degree of weathering, the lower the stability, and the greater the hazard; conversely, the farther the debris flow is, the smaller the danger.

2.3. Data Sources

By the identified evaluation indexes, the investigation reports of 310 mudslides were systematically sorted out, and GIS tools were utilized to read the DEM data and vegetation NDVI index of the Yanshan area to provide a database for the evaluation.

3. Methods

3.1. Extensional Matter Element Model

Extenics is the use of formal models to investigate the potential for the growth of things as well as the laws and methods of leading-edge innovation to eventually resolve conflicting issues, and is widely used in the fields of artificial intelligence, computers, management, control, detection, and other fields. It describes things as basic elements (thing elements) and describes the change of things N, the characteristics of things c, and the quantity value v of things about the characteristics as the three elements of thing elements, finally forming the theory and method of problem solving [53–55].

(1) Classical domain matter element model.

The debris flow susceptibility is taken as the evaluation object, and the evaluation factors with different quantitative values are selected to determine the debris flow susceptibility level to establish the classical domain. That is

$$R_{ot} = (N_{ot}, c, V_{oti}) = \begin{bmatrix} N_{ot} & c_1 & V_{ot1} \\ & c_2 & V_{ot2} \\ & \vdots & \vdots \\ & c_i & V_{oti} \end{bmatrix} = \begin{bmatrix} N_{ot} & c_1 & < a_{ot1}, b_{ot1} > \\ & c_2 & < a_{ot2}, b_{ot2} > \\ & \vdots & \vdots \\ & c_i & < a_{oti}, b_{oti} > \end{bmatrix} \tag{4}$$

where R_{ot} is the classical domain element of debris flow hazard, N_{ot} is the evaluation level of debris flow hazard, c_i is the corresponding evaluation index of debris flow hazard level, and V_{ot} is the range of quantity values taken by c_i, that is $<a_{oti},b_{oti}>$ (i = 1, 2, 3, . . ., 8).

(2) Nodal domain matter element model.

The nodal domain matter element model, or collection of the range of values of evaluation indexes, refers to the complete range of values of evaluation factors in the assessment level of debris flow danger.

$$R_p = (N_P, c, V_P) = \begin{bmatrix} N_P & c_1 & V_{P1} \\ & c_2 & V_{P2} \\ & \vdots & \vdots \\ & c_i & V_{Pi} \end{bmatrix} = \begin{bmatrix} N_P & c_1 & < a_{P1}, b_{P1} > \\ & c_2 & < a_{P2}, b_{P2} > \\ & \vdots & \vdots \\ & c_i & < a_{Pi}, b_{Pi} > \end{bmatrix} \tag{5}$$

where R_p is the nodal domain object element, N_P is the whole debris flow hazard evaluation level, V_{pi} is the quantitative range of evaluation factors, and the quantitative range of classical domain and nodal domain evaluation factors are related as follows: $<a_{ot},b_{ot}>\subset<a_{pi},b_{pi}>$ (i = 1, 2, 3, . . ., 8).

(3) Matter element model to be evaluated.

The matter element model to be evaluated is the value related to the evaluation of debris flow hazard based on the field survey or investigation for the determined evaluation factors.

$$R_j = (N_j, c, v_i) = \begin{bmatrix} N_i & c_1 & v_1 \\ & c_2 & v_2 \\ & \vdots & \vdots \\ & c_n & v_n \end{bmatrix} \tag{6}$$

where R_j is the object element to be evaluated, that is, the object element of a single debris flow; N_j is the debris flow hazard level to be evaluated, and v_i is the relevant quantity value of the debris flow hazard level.

(4) Correlation degree.

$$K_j(N) = \sum_{\substack{i=1 \\ j=1}}^{n} \alpha_i K_j(v_i) \tag{7}$$

$$K_j(v_i) = \begin{cases} \frac{\rho(v_i, v_{otj})}{\rho(v_i, v_{pj}) - \rho(v_i, v_{otj})} & (v_i \notin v_{otj}) \\ \frac{-\rho(v_i, v_{otj})}{v_{otj}} & (v_i \in v_{otj}) \end{cases} \tag{8}$$

Among them,

$$\rho(v_j, v_{otj}) = \left| v_j - \frac{a_{otj} + b_{otj}}{2} \right| - \frac{b_{otj} - a_{otj}}{2} \tag{9}$$

$$\rho(v_j, v_{Pj}) = \left| v_j - \frac{a_{Pj} + b_{Pj}}{2} \right| - \frac{b_{Pj} - a_{Pj}}{2} \tag{10}$$

$$v_{otj} = | b_{ij} - a_{ij} | \tag{11}$$

where α_i is the weight coefficient of each evaluation index and $\rho(v_i, v_{Pj})$ is the distance of the evaluation index.

3.2. Weighting Factor

In the extension evaluation of debris flow hazard, the weight coefficient of the evaluation index determines the evaluation results. Both subjective assessment and objective calculation are used to determine weight coefficients. In contrast to objective calculation, which uses mathematical formulas based on the data values of evaluation indexes and relies too heavily on the data itself and is subject to error, subjective judgment involves

ranking the evaluation indexes according to the experts' subjective understanding, which is somewhat arbitrary. Therefore, to make up for the advantages and disadvantages of the two methods, the combination of weighting is assigned through mathematical rules to obtain scientific and reasonable weight coefficients. Combined with the geological and environmental conditions of the evaluation area and evaluation indexes, the weighting coefficients are determined by calculating the weighting combination using a hierarchical analysis process and the CRITIC method.

(1) Analytic hierarchy process (AHP).

The hierarchical analysis process is a subjective decision analysis method that employs the 1–9 scale method to assess the relative value of each evaluation index by generating judgment matrices $A = (b_{ij})_{n\times n}$ to compare evaluation indexes with one another, where $b_{ij} > 0$, $b_{ij} = 1/b_{ji}$, $b_{ij} = 1(i = j)$, and $(i, j = 1, 2, 3, \ldots, 8)$. By normalizing the judgment matrix to find the eigenvector and then finding the maximum latent root $\lambda_{\max}$, a consistency test is performed to check the reasonableness of the judgment matrix [56,57].

$$AW = \lambda_{\max} W = \lambda_{\max} \begin{bmatrix} w_1 \\ w_2 \\ \vdots \\ w_n \end{bmatrix} \tag{12}$$

The formula for the consistency test of the judgment matrix is as follows:

$$C.R. = C.I./R.I. \tag{13}$$

where *C.R.* is the consistency ratio and $C.R. < 0.1$ is when the judgment matrix meets the consistency requirement; *C.I.* is the consistency index and n is the matrix order; and *R.I.* is the average random consistency index; see Table 1.

Table 1. R.I. value table.

Order *n*	RI	Order *n*	RI
1	0	6	1.26
2	0	7	1.36
3	0.58	8	1.41
4	0.89	9	1.46
5	1.12	10	1.49

(2) CRITIC empowerment method

As an objective weight calculation method, the CRITIC empowerment method is more objective and reasonable than the entropy weight method and the standard deviation method, because it takes into account the volatility and correlation of evaluation indexes and eliminates the error caused by overlapping influence factors among evaluation indexes [58]. The CRITIC empowerment method introduces contrast intensity and conflicting measures and conducts scientific evaluation based on the objective qualities of evaluation indexes themselves.

The CRITIC method calculates the steps as follows:

Step 1. Select n evaluation indicators for m evaluation objects, establish the evaluation indicator system, and construct the level matrix.

Step 2. The evaluation matrix is normalized (without negative indicators) to obtain the matrix with the following formula:

Positive indexes:

$$x_{ij} = \frac{x'_{ij} - \min(x'_{1j}, x'_{2j}, \ldots x'_{nj})}{\max(x'_{1j}, x'_{2j}, \ldots x'_{nj}) - \min(x'_{1j}, x'_{2j}, \ldots x'_{nj})} \tag{14}$$

Negative indicators:

$$x_{ij} = \frac{\max(x'_{1j}, x'_{2j}, \ldots x'_{nj}) - x'_{ij}}{\max(x'_{1j}, x'_{2j}, \ldots x'_{nj}) - \min(x'_{1j}, x'_{2j}, \ldots x'_{nj})} \tag{15}$$

Step 3. Variability of indicators. The variability of the indexes is reflected by the standard deviation of the evaluation factors.

$$\begin{cases} \overline{x}_j = \frac{1}{n} \sum\limits_{i=1}^{n} x_{ij} \\ \sigma_j = \sqrt{\frac{\sum\limits_{i=1}^{n} (x_{ij} - \overline{x}_j)}{n-1}} \end{cases} \tag{16}$$

Step 4. Indicator conflict. Conflicting indicators are represented by correlation coefficients.

$$R_j = \sum_{i=1}^{P} (1 - r_{ij}) \tag{17}$$

where the correlation coefficient r_{ij} is calculated using the Pearson correlation coefficient, and x_i and y_i are evaluation indicators, respectively.

$$r_{ij} = \frac{S_{xy}}{S_x S_y} = \frac{\sum (x_i - \overline{x})(y_i - \overline{y})}{\sqrt{\sum (x_i - \overline{x})^2} \sqrt{\sum (y_i - \overline{y})^2}} \tag{18}$$

Step 5. Amount of information. Evaluate the amount of information carried by the index.

$$C_j = \sigma_j \times R_j = \sigma_j \sum_{i=1}^{P} (1 - r_{ij}) \tag{19}$$

Step 6. Weight calculation.

$$w_j = \frac{C_j}{\sum\limits_{j=1}^{P} C_j} \tag{20}$$

(3) Game theory combination weighting

To obtain the best-combined weights, the combined weighting method organically combines the weights determined by the hierarchical analysis process and the entropy weighting method. The base weight vector set is represented as follows if M weight calculation techniques are employed to weight the evaluation indexes:

$$w_k = [w_{k1}, w_{k2}, \cdots, w_{kn}] (k = 1, 2, \cdots, M) \tag{21}$$

A linear combination of M weight vectors w is denoted as

$$w = \sum_{k=1}^{M} \gamma_k w_k^T, k = 1, 2, \cdots, M \tag{22}$$

where γ is the linear combination factor.

The objective function and constraints are constructed using game theory, and the optimal linear combination coefficients are obtained to minimize the sum of w and w_k deviations.

The objective function is as follows:

$$\min \left\| \sum_{k=1}^{M} (\gamma_k w_k^T - w_k^T) \right\|, k = 1, 2, \cdots, M \tag{23}$$

According to the principle of differentiation, the first-order derivative condition for the formula to take the minimum value is as follows:

$$\begin{bmatrix} w_1 w_1^T & w_1 w_2^T & \cdots & w_1 w_M^T \\ w_2 w_1^T & w_2 w_2^T & \cdots & w_2 w_M^T \\ \vdots & \vdots & \vdots & \vdots \\ w_M w_1^T & w_M w_2^T & \cdots & w_M w_M^T \end{bmatrix} \begin{bmatrix} \gamma_1 \\ \gamma_2 \\ \vdots \\ \gamma_M \end{bmatrix} = \begin{bmatrix} w_1 w_1^T \\ w_2 w_2^T \\ \vdots \\ w_M w_M^T \end{bmatrix} \tag{24}$$

The constraint is

$$\sum_{k=1}^{M} \gamma_k = 1 \tag{25}$$

The calculated linear combination coefficients are normalized as follows:

$$\gamma_k^* = \frac{|\gamma_k|}{\sum_{k=1}^{M} |\gamma_k|} \tag{26}$$

In turn, the optimal combination weights of evaluation indicators are obtained as follows:

$$w^* = \sum_{k=1}^{M} \gamma_k^* \cdot w_k^T \tag{27}$$

You may insert up to 5 heading levels into your manuscript, as can be seen in the "Styles" tab of this template. These formatting styles are meant as a guide; as long as the heading levels are clear, the Frontiers style will be applied during typesetting.

3.3. Evaluation Index Level and Grading

(1) debris flow hazard class.

Referring to the research results of debris flow hazard evaluation, combined with debris flow investigation data and related technical requirements, the debris flow hazard level is classified as low, medium, high, and very high hazard.

(2) Evaluation index grading.

The grading of assessment indicators is directly related to the characteristics of debris flow development, and different debris flow hazard levels correlate to varied grading of evaluation indicators. The statistical theory was used to count 310 debris flows in the study area based on the evaluation indexes on the level of debris flow danger, and the evaluation indexes were fairly graded by combining them with the real evaluation area (Figure 2).

The evaluation index data were ordered from small to large, looking for data inflection points, and the classification findings of debris flow danger evaluation indexes were calculated using the field survey (Table 2).

Table 2. Classification list of debris flow risk evaluation index values.

Evaluation Indicators	Low Risk	Medium Risk	High Risk	Extremely High Risk
Melton ratio (c_1)	0~0.10	0.10~0.30	0.30~0.50	0.50~1.20
Basin elongation (c_2)	0.60~40.00	0.30~0.60	0.10~0.30	0~0.10
Basin height difference rate (c_3)	0~0.10	0.10~0.20	0.20~0.30	0.30~5.0
Slope gradient (°) (c_4)	0~15	15~30	30~40	40~90
Loose material reserves (10^4 m^3) (c_5)	0~1.0	1.0~5.0	5.0~10.0	10.0~150
NDVI vegetation index (c_6)	0.75~1.00	0.6~0.75	0.4~0.6	0~0.4
Average annual precipitation (mm) (c_7)	0~450	450~550	550~620	620~800
Distance from structure (10^3 m) (c_8)	5~25	2.5~5	1.0~2.5	0~1.0

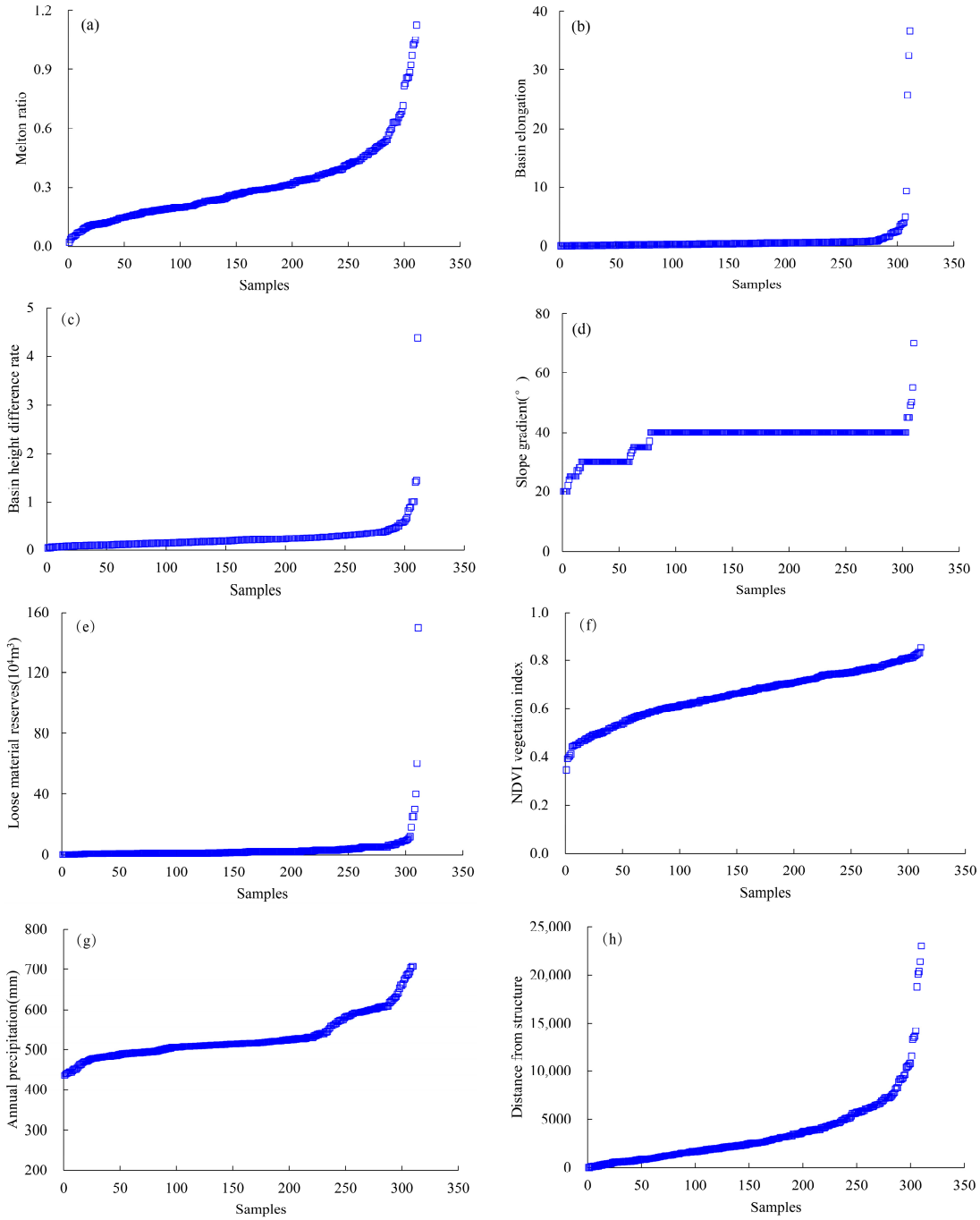

Figure 2. Statistics of evaluation indicators. (**a**) Melton ratio; (**b**) basin elongation; (**c**) basin height difference rate; (**d**) slope gradient; (**e**) loose material reserves; (**f**) NDVI vegetation index; (**g**) average annual precipitation; and (**h**) distance from structure.

(3) Dimensionless evaluation index

To eliminate the calculation errors caused by different units among the evaluation indicators, the evaluation indicator values in Table 2 are dimensionless using the polarization regularization method, and the calculation formula is shown in Equation (28), and the evaluation indicator values are between [0, 1], as shown in Table 3.

$$y_i = \frac{x_i - x_{\min}}{x_{\max} - x_{\min}} \tag{28}$$

Table 3. Debris flow hazard assessment index value classification list (dimensionless).

Evaluating Indicator	Low Risk	Medium Risk	High Risk	Very High Risk
Melton ratio (c_1)	0~0.0833	0.0833~0.25	0.25~0.4167	0.4167~1
Basin elongation (c_2)	0.015~1	0.0075~0.015	0.0075~0.0025	0.0025~0
Basin height difference rate (c_3)	0~0.02	0.02~0.04	0.04~0.06	0.06~1
Slope gradient (c_4)	0~0.1667	0.1667~0.3333	0.3333~0.4444	0.4444~1
Loose material reserves (c_5)	0~0.0067	0.0067~0.0333	0.0333~0.0667	0.0667~1
NDVI vegetation index (c_6)	0.75~1	0.6~0.75	0.4~0.6	0~0.4
Average annual precipitation (c_7)	0~0.5625	0.5625~0.6875	0.6875~0.775	0.775~1
Distance from structure (c_8)	0.2~1	0.1~0.2	0.04~0.1	0~0.04

4. Results

Three distinct but interconnected steps make up the topological evaluation of the risk of mudslides: weight coefficient computation, evaluation index selection and grading, and topological evaluation. The evaluation indices are established, the classical domain object element, the nodal domain object element, and the object element that will be evaluated are built using the theory of topology, reasonable weight coefficients are established, and the correlation function is introduced, the maximum value of which will be used to determine the hazard grade (Figure 3). It should be noted that these three parts are independent of each other again. The selection of evaluation indexes is mainly determined according to the expert's knowledge of the influence factors of a mudslide; the game theory idea is only an optimal combination of the results obtained from different weight coefficient calculation methods, which has no relationship with the method itself; and the topological evaluation uses the most suitable evaluation indexes and the optimal weight coefficients, which improves the accuracy of the evaluation results.

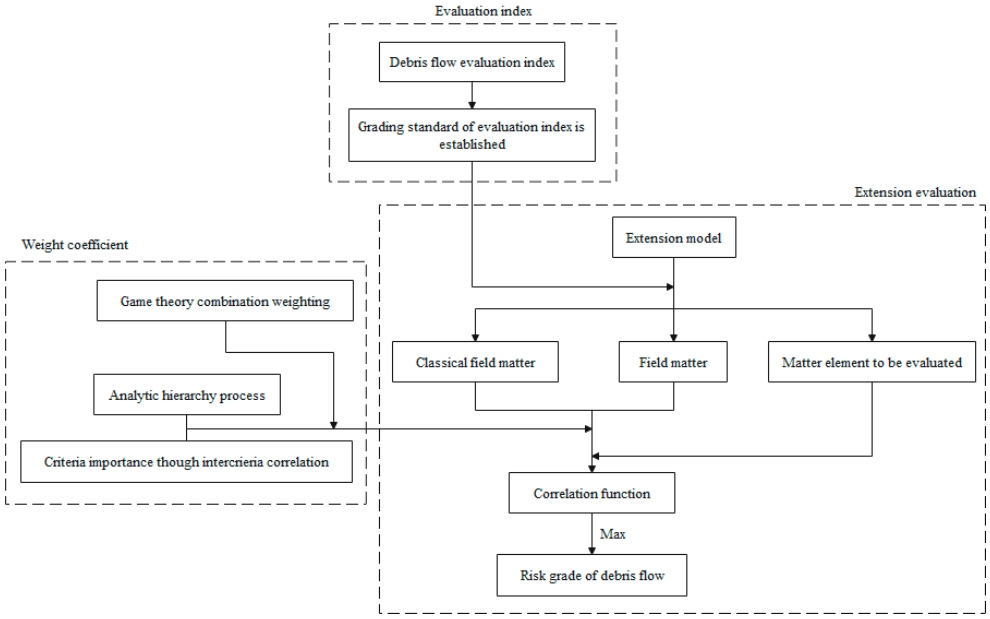

Figure 3. Technical route of debris flow hazard evaluation.

4.1. Topological Model

The debris flow hazard classical domain matter element model and nodal domain matter element model are determined by using the extension matter element model.

Classical domain matter element model:

$$R_{ot1} = \begin{bmatrix} N_{ot1} & c_1 & <0.0000, 0.0833> \\ & c_2 & <0.0150, 1.0000> \\ & c_3 & <0.0000, 0.0200> \\ & c_4 & <0.0000, 0.1667> \\ & c_5 & <0.0000, 0.0067> \\ & c_6 & <0.7500, 1.0000> \\ & c_7 & <0.0000, 0.5625> \\ & c_8 & <0.2000, 1.0000> \end{bmatrix} \quad R_{ot2} = \begin{bmatrix} N_{ot2} & c_1 & <0.0833, 0.2500> \\ & c_2 & <0.0075, 0.0150,> \\ & c_3 & <0.0200, 0.0400> \\ & c_4 & <0.1667, 0.3333> \\ & c_5 & <0.0067, 0.0333> \\ & c_6 & <0.6000, 0.7500> \\ & c_7 & <0.5625, 0.6875> \\ & c_8 & <0.1000, 0.2000> \end{bmatrix}$$

$$R_{ot3} = \begin{bmatrix} N_{ot3} & c_1 & <0.2500, 0.5000> \\ & c_2 & <0.0025, 0.0150> \\ & c_3 & <0.0400, 0.0800> \\ & c_4 & <0.3333, 0.4444> \\ & c_5 & <0.0333, 0.0667> \\ & c_6 & <0.4000, 0.6000> \\ & c_7 & <0.6875, 0.8125> \\ & c_8 & <0.0200, 0.1000> \end{bmatrix} \quad R_{ot4} = \begin{bmatrix} N_{ot4} & c_1 & <0.5000, 1.0000> \\ & c_2 & <0.0000, 0.0025> \\ & c_3 & <0.0800, 1.0000> \\ & c_4 & <0.4444, 1.0000> \\ & c_5 & <0.0667, 1.0000> \\ & c_6 & <0.0000, 0.4000> \\ & c_7 & <0.8125, 1.0000> \\ & c_8 & <0.0000, 0.0200> \end{bmatrix}$$

Nodal domain matter element model:

$$R_P = \begin{bmatrix} N_P & c_1 & <0.0000, 1.0000> \\ & c_2 & <0.0000, 1.0000> \\ & c_3 & <0.0000, 1.0000> \\ & c_4 & <0.0000, 1.0000> \\ & c_5 & <0.0000, 1.0000> \\ & c_6 & <0.0000, 1.0000> \\ & c_7 & <0.0000, 1.0000> \\ & c_8 & <0.0000, 1.0000> \end{bmatrix}$$

4.2. Weighting Coefficient

Based on the hierarchical analysis process, the degree of contribution of evaluation indexes to the risk of the debris flow was determined through the debris flow survey in the study area combined with the existing survey results, the judgment matrix $A = (c_{ij})_{8\times8}$ was constructed, and the weight coefficients were calculated according to Equation (12) (Table 4), where $C.R. \leq 0.1$ met the requirements.

Table 4. Calculation results of the weight of the hierarchical analysis process.

Evaluation Indicators	c_1	c_2	c_3	c_4	c_5	c_6	c_7	c_8
Weights	0.1015	0.0677	0.2030	0.0761	0.1585	0.0507	0.3044	0.0381

Using the CRITIC weighting method, objective weight coefficients were determined (Table 5). It can be seen that the greater the variability of the indicators, the greater the weight; the stronger the correlation between the indicators, the lower the conflict and the smaller the weight.

Based on game-theoretic ideas, the minimum first-order derivatives are derived and normalized to determine the optimal combination weight coefficients using Equations (24)–(26) (Table 6).

$$\begin{cases} 0.1837w_1 + 0.1225w_2 = 0.1837 \\ 0.1225w_1 + 0.1492w_2 = 0.1492 \end{cases}$$

Table 5. Calculation results of CRITIC method weights.

Evaluation Indicators	c_1	c_2	c_3	c_4	c_5	c_6	c_7	c_8
Variability of indicators	0.170	0.087	0.068	0.107	0.065	0.203	0.196	0.152
Conflicting indicators	6.379	7.295	6.826	6.963	6.827	8.188	6.975	7.018
Amount of information	1.086	0.633	0.466	0.742	0.445	1.665	1.364	1.067
Weighting factor	0.1454	0.0848	0.0623	0.0993	0.0596	0.223	0.1827	0.1429

Table 6. Game theory portfolio weighting coefficients.

Evaluation Indicators	c_1	c_2	c_3	c_4	c_5	c_6	c_7	c_8
Analytic hierarchy process	0.1015	0.0677	0.2030	0.0761	0.1585	0.0507	0.3044	0.0381
CRITIC method	0.1454	0.0848	0.0623	0.0993	0.0596	0.2230	0.1827	0.1429
The optimal combination weighting factor	$w_1^* = 0.6509$, $w_2^* = 0.3491$							
Portfolio weights	0.1168	0.0737	0.1539	0.0842	0.1240	0.1108	0.2619	0.0747

4.3. Matter-Element Model to Be Evaluated

The 310 debris flows in the evaluation area are formalized, four debris flow potential sites are selected as objects to be evaluated, norming to the evaluation index grading standard, and the matter element model to be evaluated is constructed. See the formula below

$$R_1 = \begin{bmatrix} N_1 & c_1 & 0.1976 \\ & c_2 & 0.0005 \\ & c_3 & 0.0429 \\ & c_4 & 0.0233 \\ & c_5 & 0.3333 \\ & c_6 & 0.4758 \\ & c_7 & 0.5564 \\ & c_8 & 0.2275 \end{bmatrix} \quad R_2 = \begin{bmatrix} N_2 & c_1 & 0.2006 \\ & c_2 & 0.0022 \\ & c_3 & 0.0465 \\ & c_4 & 0.0067 \\ & c_5 & 0.4444 \\ & c_6 & 0.6609 \\ & c_7 & 0.6379 \\ & c_8 & 0.1274 \end{bmatrix}$$

$$R_3 = \begin{bmatrix} N_3 & c_1 & 0.1860 \\ & c_2 & 0.0024 \\ & c_3 & 0.0357 \\ & c_4 & 0.0200 \\ & c_5 & 0.4444 \\ & c_6 & 0.7883 \\ & c_7 & 0.7506 \\ & c_8 & 0.0375 \end{bmatrix} \quad R_4 = \begin{bmatrix} N_4 & c_1 & 0.5270 \\ & c_2 & 0.0127 \\ & c_3 & 0.0552 \\ & c_4 & 0.0133 \\ & c_5 & 0.4444 \\ & c_6 & 0.7203 \\ & c_7 & 0.7877 \\ & c_8 & 0.0842 \end{bmatrix}$$

The correlation function is used to evaluate the debris flow hazard level at four locations, and the maximum value of the correlation is used as the debris flow hazard level (Equation (29)).

$$K(N) = \max\{K_j(N)\} \quad (j = 1, 2, 3, 4) \tag{29}$$

It can be seen that the danger level of 1# and 2# debris flows is medium danger, 3# debris flow danger is high, and 4# debris flow danger is very high (Table 7). After field verification and combined with relevant technical standards, it is believed that the evaluation combination is more scientific and reasonable, which is in line with reality.

Table 7. List of correlations of debris flow hazard evaluation.

Number	Low Risk	Medium Risk	High Risk	Extremely High Risk
1#	−0.2524	−0.2076	−0.2398	−0.2708
2#	−0.3152	−0.0071	−0.1815	−0.2710
3#	−0.3330	−0.2220	−0.1679	−0.2461
4#	−0.3713	−0.2645	−0.1726	−0.1247

5. Discussion

5.1. Evaluation Results

When conducting an extension evaluation, the evaluation results are determined by introducing the correlation degree after assigning the evaluation indexes to the system once and using the maximization principle, which is consistent with the evaluation principle of high but not low in geological disaster prevention and control management [59–61]. The information quantity method to risk evaluation is to assign weights to evaluation indicators twice to determine the evaluation results: first to carry out susceptibility evaluation and again to superimpose predisposing factors to determine the evaluation results, which has the advantage of extracting the informativeness of a large number of data samples and obtaining the indicators of the samples in different regions [62,63]. The pertinent technical standards are the subjectively based qualitative assessment of debris flow hazards, which is mainly subjective and harmonizes the evaluation indicators and grades. Field validation is based on the consideration of rainfall factors, the source of debris flow, height difference, slope, and other factors to determine the evaluation results of the comprehensive analysis; it is also based on qualitative evaluation, a more intuitive understanding of the debris flow assessment.

From Table 8, it can be seen that among multiple evaluation methods, the extension evaluation method is consistent with relevant technical standards and field verification results in the risk assessment results of debris flow from 1# to 4#. The evaluation results of debris flow #1 differ from those of the information quantity evaluation, which can be understood from two perspectives. First, the hierarchical analysis process is used to calculate weight coefficients in information quantity evaluation, which ignores the correlation between evaluation indexes and amplifies the weight coefficients of significant evaluation indexes. Second, the information quantity evaluation process is assigned twice, and the assignment becomes too subjective when adding rainfall factors. As extension evaluation eliminates mutuality and contradiction among evaluation indicators, it is more methodical and rational in allocating weights than other evaluation systems.

Table 8. Comparison of debris flow hazard evaluation results.

Number	Extension Evaluation	Information Quantity Evaluation	Related Technique Standard	Field Check
1#	Medium risk	Low risk	Medium risk	Medium risk
2#	Medium risk	Medium risk	Medium risk	Medium risk
3#	high risk	high risk	high risk	high risk
4#	Extremely high risk	Extremely high risk	Extremely high risk	Extremely high risk

The geological and environmental circumstances are more complex for debris flow #1. According to the characteristics of debris flow development, the debris flow lithology is rhyolite of the Mesozoic Jurassic Zhangjiakou Formation; the watershed area is 0.4 km^4, the relative height difference is 150 m, the volume of loose material reserves is approximately 3.5×10^4 m^3, the average slope of both sides of the gully valley is 30°, the debris siltation in the gully is obvious, the circulation area is slightly blocked, and the rainfall in the study area from 2016 to 2021 is large. From this, it is inferred that the hazard class of mudslide #1 is medium hazardous(Figure 4). It is concluded that the extension evaluation method

can be used to assess the risk posed by debris flows and that the evaluation's findings are accurate and logical.

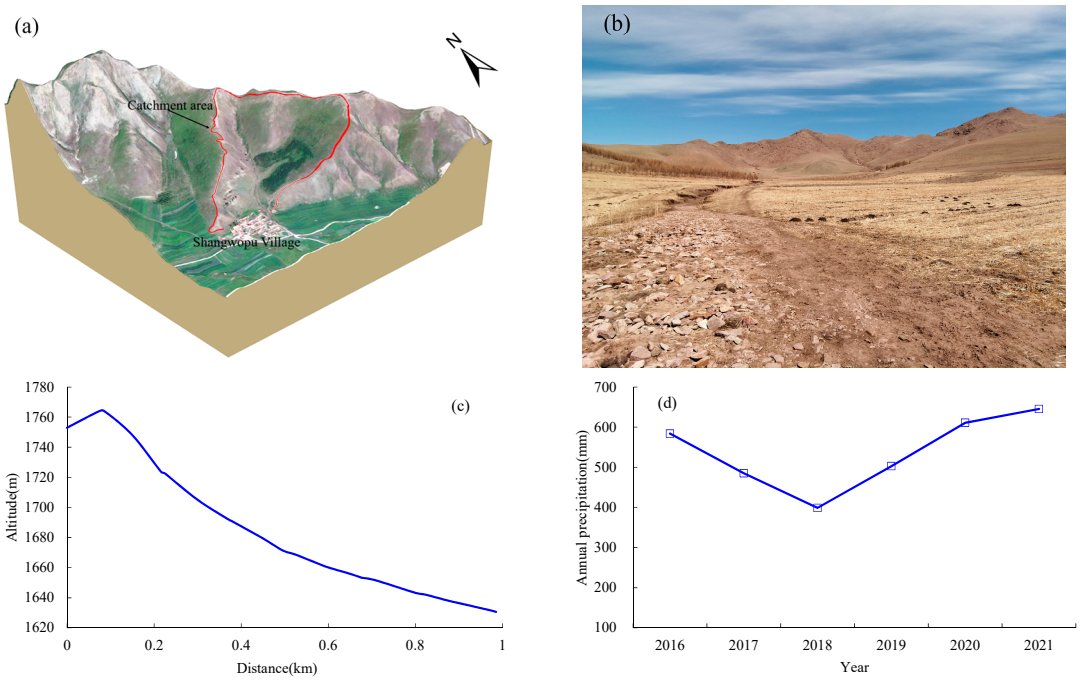

Figure 4. Features of 1# debris flow development. (**a**) three-dimensional image map of the debris flow; (**b**) debris flow site survey photos; (**c**) terrain height difference of debris flow; and (**d**) average annual precipitation.

5.2. Evaluation Method Optimization

The determination and grading of evaluation indexes, calculating weight coefficients, and creating an extension model and correlation function are the three steps that make up the entire extension evaluation process. The assessment indexes serve as the fundamental building blocks of the entire evaluation. They help establish if the evaluation method adequately and objectively addresses the characteristics of debris flow development, and the scientific and reasonable grading has an impact on how the extension evaluation is classified. The importance of each evaluation index is reflected in the weight coefficient, which has a significant impact on the evaluation's outcomes. The core of the evaluation is the development of the extension model, and the introduction of the correlation degree function determines the evaluation grade with the maximization principle, which is consistent with the principle of high and not low in the assessment of geological disasters. So, it is evident that field and inter-field verification of the evaluation outcomes is necessary.

Mostly, lithology, watershed area, slope angle, elevation, and other indicators of debris flow development characteristics are used in debris flow susceptibility or hazard evaluation indexes [64–67], or they are used to analyze debris flow hazards from large watersheds. These indicators reflect debris flow development characteristics but cannot completely reflect the changing state of debris flow, especially individual debris flow gullies, whose development elements cannot be fully revealed [68–73]. Therefore, the authors believe that within a small watershed with a county as a unit, rainfall, topography, vegetation cover, and loose material reserves have a greater influence on debris flow. The introduction of indicators like the melton ratio, basin elongation, and basin height difference rate, which reflect the development state of debris flow from various perspectives based on ensuring the independence among indicators, is very meaningful for the evaluative process [52]. Furthermore, field verification of the evaluation results is required in order to scientifically revise the evaluation index grading criteria because the evaluation index grading criteria

are not fixed and are graded on the average delineation, which is related to the contribution rate of each evaluation index to the debris flow hazard in the evaluation basin [74,75].

The weighting coefficient is a correction of the importance of the evaluation indicators, which also needs to be adjusted, and is related to the extent to which the evaluation indicators contribute to the risk in the evaluation basin. To determine the weighting coefficient comprehensively, it is important to take into account both the knowledge of experienced experts on the evaluation indicators and the objective properties of the evaluation indicators.

The development of the extension model is intimately tied to the grading of the evaluation index, which has a direct impact on the correctness of the assessment outcomes. The data basis for the correlation degree function is provided by the construction of the classical domain, the nodal domain, and the object elements to be assessed, and the evaluation grade is established according to the maximization principle.

It is clear that there are logical connections between the evaluation indices, weighting coefficients, and extension matter elements. The development of the extension model is directly impacted by reasonable evaluation indexes and optimal weighting coefficients, and the verification of the extension evaluation results optimizes and adjusts the evaluation indexes and weighting coefficients. Accordingly, the entire evaluation process must be carried out based on mastering the geological environment conditions of the evaluation area and adapting the evaluation process to changes in the subsurface.

5.3. Application of Evaluation Methods

After the Section 5.1 reviews, the extension evaluation's findings satisfy the requirements for reality, practicability, and science and can be used for debris flow hazard evaluation, where the use of GIS, RS, and other geographic information technology increases the efficiency and precision of debris flow hazard evaluation [76–79]. Thus, using GIS as a platform, the debris flow gully unit is divided by county or small watershed, the basic geological information of the debris flow gully unit is mastered through a high-precision survey, the evaluation index grading standard is determined using the GIS information collection function, the object element model is constructed, technical experts are organized to qualitatively weight the evaluation index, and the objective weights of the evaluation index determined by CRITIC assign are combined, establishing the correlation degree function through GIS operation function, and determining the evaluation grade by the principle of maximum value. The weight factors and evaluation findings must be modified in a timely manner if evaluation indicators like rainfall and loose accumulation change. In addition, the technique may be used to assess rockfall hazards, and the slope units are split by GIS to conduct the topological evaluation.

Professional technicians integrating the mudslide hazard evaluation method using GIS for secondary development, creating a set of evaluation procedures using GIS tools, choosing evaluation indices for various regions in conjunction with work experience, automatically allocating weight coefficients to complete the evaluation by the game-theoretic hod, and evaluating the system and adjusting the results can possibly take 3–5 days. A mudslide in the mountainous region of western Jixi was chosen to further confirm the validity and applicability of the method. The optimal weight coefficients were then determined by the set evaluation indexes, and it was discovered that the mudslide's danger level was medium, which was consistent with the results of the on-site investigation.

6. Conclusions

Based on the game theory concept, the combination of the hierarchical analysis process and CRITIC method empowerment and the use of the extension theory system to carry out debris flow hazard evaluation is largely in line with reality. The method is scientific and feasible, which provides a basis for geological disaster meteorological risk warning projects and provides a reference for local government geological disaster prevention and control work. The following are the key findings:

(1) The development characteristics and distribution rules of debris flows in Jidong Yanshan's mountainous areas were systematically sorted; the factors influencing the development of debris flows, such as topography and geomorphology, stratigraphic lithology, geological structure, and rainfall, were summarized and analyzed; the evaluation indexes, such as melton ratio, vegetation NDVI index, basin elongation, loose material reserves, basin height difference rate, slope, average annual precipitation, and distance from structure, were identified; the evaluation indexes of 310 debris flows were analyzed graphically using statistics; and the grading of evaluation indexes and the establishment of grading criteria were carried out;

(2) The weight coefficients from both subjective and objective aspects were calculated, respectively, using the hierarchical analysis process and the CRITIC method. The ideal weight coefficients were then obtained by combining the weight assignments with the use of game theory concepts;

(3) The classical domain, nodal domain, and metamodel of the object to be evaluated were built using extension theory by the evaluation index grading criteria. The evaluation grade was determined by the correlation degree function with the maximum principle, and the comparison with other methods was verified. The evaluation results were found to be applicable, and the method was found to be workable.

Author Contributions: H.L. and X.Z. (Xing Zhai) were responsible for the analysis and writing of the manuscript; X.B. was responsible for the review and revision of the manuscript; X.Z. (Xiaolong Zhu) and C.L. were responsible for the computational part; K.L. was responsible for the field verification; and J.Z. was responsible for the supervision and proofreading. Q.W. conducted an inspection work. All authors have read and agreed to the published version of the manuscript.

Funding: This work was supported by the Geological Survey Project of China Geological Survey [WT2019078B] and the Key Laboratory Project of Geological Resources and Environment Monitoring and Protection in Hebei Province [JCYKT202004].

Data Availability Statement: The data used to support the findings of this study are included in the manuscript.

Conflicts of Interest: The authors declare no conflict of interest.

References

1. Kang, Z.; Li, C.; Ma, A.; Luo, J. *Study on Debris Flow in China*; Science Press: Beijing, China, 2004; pp. 1–15.
2. Sebastián, F.D.; Valérie, B.; Noelia, C. The twin catastrophic flows occurred in 2014 at Ambato Range (28°09′–28°20′ S), Catamarca Province, Northwest Argentina. *J. S. Am. Earth Sci.* **2021**, *106*, 103086.
3. Chao, K.; Dave, C. Investigation of erosion characteristics of debris flow based on historical cases. *Eng. Geol.* **2022**, *306*, 106767.
4. Gisonni, C. Debris flow: Mechanics, prediction and countermeasures. *J. Hydraul. Res.* **2008**, *46*, 144. [CrossRef]
5. He, Z. Development characteristics of debris flow and its influence on migration site. *BioTechnol. Indian J.* **2014**, *10*, 8818–8821.
6. Okubo, S.; Ikeya, H.; Ishikawa, Y.; Yamada, T. Development of new methods for countermeasures against debris flows. *Recent Dev. Debris Flows* **2007**, *64*, 166–185.
7. Tang, C.; van Asch, T.W.; Chang, M.; Chen, G.Q.; Zhao, X.H.; Huang, X.C. Catastrophic debris flows on 13 August 2010 in the Qingping area, southwestern China: The combined effects of a strong earthquake and subsequent rainstorms. *Geomorphology* **2012**, *139*, 559–576. [CrossRef]
8. Breien, H.; De Blasio, F.V.; Elverhøi, A.; Høeg, K. Erosion and morphology of a debris flow caused by a glacial lake outburst flood, Western Norway. *Landslides* **2008**, *5*, 271–280. [CrossRef]
9. Fiorillo, F.; Wilsion, R.C. Rainfall induced debris flows in pyroclastic deposits, Campania (Southern Italy). *Eng. Geol.* **2004**, *75*, 263–289. [CrossRef]
10. Shang, Y. Geological and Geomorphologic Disasters and Disaster Prevention and Reduction in Hebei Province. *J. Catastrophol.* **1999**, *14*, 33–38.
11. Bentivenga, M.; Bellanova, J.; Calamita, G.; Capece, A.; Cavalcante, F.; Gueguen, E.; Guglielmi, P.; Murgante, B.; Palladino, G.; Perrone, A.; et al. Geomorphological and geophysical surveys with InSAR analysis applied to the Picerno earth flow (southern Apennines, Italy). *Landslides* **2021**, *18*, 471–483. [CrossRef]
12. Carolin, K.; Patrick, O.; Jasper, M.; Claudio, F.S.; Christoph, M.; Michael, S.; Michael, K. A 4000-year debris flow record based on amphibious investigations of fan delta activity in Plansee (Austria, Eastern Alps). *Earth Surf. Dyn.* **2021**, *9*, 1481–1503.

13. Zhou, G.; Lyu, L.; Xu, M.; Ma, C.; Wang, Y.; Wang, Y.; Wang, Z.; Stoffel, M. Assessment of check dams and afforestation in mitigating debris flows based on dendrogeomorphic reconstructions, field surveys and semi-empirical models. *Catena* **2023**, *232*, 107434. [CrossRef]
14. Teemu, H.; Peter, F.; Philip, S.; Philipp, R.; Ansgar, W.; Andreas, V.; Frieder, E. Multi-Methodological Investigation of the Biersdorf Hillslope Debris Flow (Rheinland-Pfalz, Germany) Associated to the Torrential Rainfall Event of 14 July 2021. *Geosciences* **2022**, *12*, 245.
15. Seph, B.Y.; Gi, K.M.; Han, P.K.; Keun, O.T.; Hyun, S.J. Development of the Damage Investigation Item to Debris Flow using the Delphi Method. *J. Korean Soc. Saf.* **2016**, *31*, 41–48.
16. Nejc, B.; Jošt, S.; Matej, M.; Timotej, J.; Jernej, J.; Tina, P.; Matjaž, M. Investigation of potential debris flows above the Koroška Bela settlement, NW Slovenia, from hydro-technical and conceptual design perspectives. *Landslides* **2021**, *18*, 3891–3906.
17. Peng, B.; Xiao, X.; Zhao, B.; Li, H. Application of digital twins in high precision geological hazard survey and prevention in Beijing. *Int. Arch. Photogramm. Remote Sens. Spat. Inf. Sci.* **2022**, *XLVIII-3/W1-2022*, 39–44. [CrossRef]
18. Chalk, C.M.; Peakall, J.; Keevil, G.; Fuentes, R. Spatial and temporal evolution of an experimental debris flow, exhibiting coupled fluid and particulate phases. *Acta Geotech.* **2021**, *17*, 965–979. [CrossRef]
19. Baselt, I.; de Oliveira, G.Q.; Fischer, J.-T.; Pudasaini, S.P. Evolution of stony debris flows in laboratory experiments. *Geomorphology* **2021**, *372*, 107431. [CrossRef]
20. van Asch, T.W.J.; Yu, B.; Hu, W. The Development of a 1-D Integrated Hydro-Mechanical Model Based on Flume Tests to Unravel Different Hydrological Triggering Processes of Debris Flows. *Water* **2018**, *10*, 950. [CrossRef]
21. Haruka, T.; Yoshinori, S.; Norifumi, H.; Christopher, G.; Yuichi, S. Multi-decadal changes in the relationships between rainfall characteristics and debris-flow occurrences in response to gully evolution after the 1990–1995 Mount Unzen eruptions. *Earth Surf. Process. Landf.* **2021**, *46*, 2141–2162.
22. Rickenmann, D. Debris-Flow Hazard Assessment and Methods Applied in Engineering Practice. *Int. J. Eros. Control Eng.* **2016**, *9*, 80–90. [CrossRef]
23. Kim, S.; Lee, H.-J. Assessment of Risk Due to Debris Flow and Its Application to a Marine Environment. *Mar. Georesour. Geotechnol.* **2015**, *33*, 572–578. [CrossRef]
24. Roberti, G.; Friele, P.; van Wyk de Vries, B.; Ward, B.; Clague, J.J.; Perotti, L.; Giardino, M. Rheological evolution of the Mount Meager 2010 debris avalanche, southwestern British Columbia. *Geosphere* **2017**, *13*, 369–390. [CrossRef]
25. Eldeen, M.T. Predisaster physical planning:intergration of disasterrisk analys is into physical planning acase study in Tunisia. *Disasters* **1980**, *4*, 211–222. [CrossRef] [PubMed]
26. Hollingsworth, R.; Kovacs, G.S. Soil Slumps and Debris Flows: Prediction and Protection. *Environ. Eng. Geosci.* **1981**, *xviii*, 17–28. [CrossRef]
27. Ohmori, H.; Hirano, M. Magnitude frequency and geomorphological significance of rocky debris flows, landcreep and the collapse of steep slopes. *Z. Fur Geomorphol.* **1988**, *67*, 55–65.
28. Carrara, A.; Cardinali, M.; Detti, R.; Guzzetti, F.; Pasqui, V.; Reichenbach, P. GIS techniques and statistical models in evaluating landslide hazard. *Earth Surf. Process. Landf.* **1991**, *16*, 427–445. [CrossRef]
29. Carrara, A. Uncertainty in Assessing Landslide Hazard and Risk. In *Prediction and Perception of Natural Hazards*; Springer: Berlin/Heidelberg, Germany, 1992; pp. 101–109.
30. Ran, L.M.; Myoung, C.J.; Sic, Y.H. Quantitative Risk Analysis of Debris Flow Disasters in Urban Area Using Geographic Information System. *Sens. Mater.* **2020**, *32*, 4573–4586.
31. Pallàs, R.; Vilaplana, J.M.; Guinau, M.; Falgàs, E.; Alemany, X.; Muñoz, A. A pragmatic approach to debris flow hazard mapping in areas affected by Hurricane Mitch: Example from NW Nicaragua. *Eng. Geol.* **2003**, *72*, 57–72. [CrossRef]
32. Kim, H.-S.; Chung, C.-K.; Kim, S.-R.; Kim, K.-S. A GIS-Based Framework for Real-Time Debris-Flow Hazard Assessment for Expressways in Korea. *Int. J. Disaster Risk Sci.* **2016**, *7*, 293–311. [CrossRef]
33. Joong, R.H.; Hwan, S.J.; Seok, S.H.; Hong, K.G.; Woo, L.S. A Model for Evaluation of Debris Flow Risk in a Watershed. *J. Korean Soc. Hazard Mitig.* **2012**, *12*, 67–76.
34. Gomez, C.; Purdie, H. Point cloud technology and 2D computational flow dynamic modeling for rapid hazards and disaster risk appraisal on Yellow Creek fan, Southern Alps of New Zealand. *Prog. Earth Planet. Sci.* **2018**, *5*, 50. [CrossRef]
35. Monia, C.; Valeria, M.; Vania, M.; Nicola, S.; Enrico, M. Rockfall and Debris Flow Hazard Assessment in the SW Escarpment of Montagna del Morrone Ridge (Abruzzo, Central Italy). *Water* **2020**, *12*, 1206.
36. Horton, A.J.; Hales, T.C.; Ouyang, C.; Fan, X. Identifying post-earthquake debris flow hazard using Massflow. *Eng. Geol.* **2019**, *258*, 105134. [CrossRef]
37. Yongde, K.; Jingming, H.; Yu, T.; Baoshan, S. A Hydrodynamic-Based Robust Numerical Model for Debris Hazard and Risk Assessment. *Sustainability* **2021**, *13*, 7955.
38. Vasu, N.N.; Lee, S.-R.; Lee, D.-H.; Park, J.; Chae, B.-G. A method to develop the input parameter database for site-specific debris flow hazard prediction under extreme rainfall. *Landslides* **2018**, *15*, 1523–1539. [CrossRef]
39. Kumar, D.R.; Prasanna, K.D.; Phillippe, M.J. Runout modelling and hazard assessment of Tangni debris flow in Garhwal Himalayas, India. *Environ. Earth Sci.* **2021**, *80*, 338.
40. Bao, G.X.; Wang, L.; Hong, Q. The Risk Assessment of Debris Flow in the Duba River Watershed Using Intuitionistic Fuzzy Sets: TOPSIS Model. *Math. Probl. Eng.* **2022**, *2022*, 2031907.

41. Seungjun, L.; Hyunuk, A.; Minseok, K.; Hyuntaek, L.; Yongseong, K. A Simple Deposition Model for Debris Flow Simulation Considering the Erosion–Entrainment–Deposition Process. *Remote Sens.* **2022**, *14*, 1904.
42. Hualin, C.; Yu, H.; Weijie, Z.; Qiang, X. Physical process-based runout modeling and hazard assessment of catastrophic debris flow using SPH incorporated with ArcGIS: A case study of the Hongchun gully. *Catena* **2022**, *212*, 106052.
43. Gu, X.B.; Shao, J.L.; Wu, S.T.; Wu, Q.H.; Bai, H. The Risk Assessment of Debris Flow Hazards in Zhouqu Based on the Projection Pursuit Classification Model. *Geotech. Geol. Eng.* **2021**, *40*, 1267–1279. [CrossRef]
44. Nie, Y.; Li, X.; Xu, R. Dynamic hazard assessment of debris flow based on TRIGRS and flow-R coupled models. *Stoch. Environ. Res. Risk Assess.* **2021**, *36*, 97–114. [CrossRef]
45. Ali, S.; Haider, R.; Abbas, W.; Basharat, M.; Reicherter, K. Empirical assessment of rockfall and debris flow risk along the Karakoram Highway, Pakistan. *Nat. Hazards* **2021**, *106*, 2437–2460. [CrossRef]
46. Gomez, H.; Kavzoglu, T. Assessment of shallow landslide susceptibility using artificial neuralnetworks in Jabonosa River Basin, Venezuela. *Eng. Geol.* **2004**, *78*, 11–27. [CrossRef]
47. Li, J.; Lv, Y. Risk Assessment of Debris Flow in Huyugou River Basin Based on Machine Learning and Mass Flow. *Mob. Inf. Syst.* **2022**, *2022*, 9751504. [CrossRef]
48. Jacob, S.; Nils, G.; Ioan, N.; Emil, P. Probabilistic Investigation and Risk Assessment of Debris Transport in Extreme Hydrodynamic Conditions. *J. Waterw. Port Coast. Ocean. Eng.* **2018**, *144*, 4017039.
49. Li, Q.; Huang, D.; Pei, S.; Qiao, J.; Wang, M. Using Physical Model Experiments for Hazards Assessment of Rainfall-Induced Debris Landslides. *J. Earth Sci.* **2021**, *32*, 1113–1128. [CrossRef]
50. Melton, M.A. The Geomorphic and Paleoclimatic Significance of Alluvial Deposits in Southern Arizona: A Reply. *J. Geol.* **1966**, *74*, 102–106. [CrossRef]
51. Schumm, S.A. Evolution of Drainage Systems and Slopes in Badlands at Perth Amboy, New Jersey. *Geol. Soc. Am. Bull.* **1956**, *67*, 597–646. [CrossRef]
52. Zhang, S.; Wu, G.; Zhang, Q.; Gao, F. Debris-flow susceptibility assessment using the characteristic factors of a catchment. *Hydrogeol. Eng. Geol.* **2018**, *45*, 142–149.
53. Cai, W. The extension set and non-compatible problems. *Sci. Explor. China* **1983**, *17*, 83–97.
54. Cai, W. Introduction of extenics. *Syst. Eng.-Theory Pract. China* **1998**, *18*, 76–84.
55. Cai, W.; Yang, C.Y.; Wang, G.H. A new cross subject-extenics. *Bull. Natl. Nat. Sci. Found. China* **2004**, *18*, 268–272.
56. Saaty, T.L. How to Make a Decision: The Analytic Hierarchy Process. *Aestimum* **1994**, *48*, 9–26.
57. Saaty, T.L. The modern science of multicriteria decision making and its practical applications: The AHP/ANP approach. *Oper. Res.* **2015**, *55*, 79–81. [CrossRef]
58. Diakoulaki, D.; Mavrotas, G.; Papayannakis, L. Determining objective weights in multiple criteria problems: The critic method. *Comput. Oper. Res.* **1995**, *22*, 763–770. [CrossRef]
59. Mehmood, Q.; Qing, W.; Chen, J.; Yan, J.; Ammar, M.; Rahman, G. Susceptibility Assessment of Single Gully Debris Flow Based on AHP and Extension Method. *Civ. Eng. J.* **2021**, *7*, 953–973. [CrossRef]
60. Xu, W.; Zhang, X.; Zou, Y.; Zhang, C.; Liu, S. Debris Flow Risk Mapping Based on GIS and Extenics. *Nat. Hazards Earth Syst. Sci. Discuss.* **2018**, *147*, 1–15.
61. Niu, C.-C.; Wang, Q.; Chen, J.-P. Debris-flow hazard assessment based on stepwise discriminant analysis and extension theory. *Q. J. Eng. Geol. Hydrogeol.* **2014**, *47*, 211–222. [CrossRef]
62. Fang, J.; Quan, H. Risk Analysis of Debris Flow hazardsin Yanbian Prefecture Based on Information Quantity Method. *IOP Conf. Ser. Earth Environ. Sci.* **2019**, *300*, 22051. [CrossRef]
63. Xu, W.; Yu, W.; Jing, S.; Zhang, G.; Huang, J. Debris flow susceptibility assessment by GIS and information value model in a large-scale region, Sichuan Province (China). *Nat. Hazards* **2013**, *65*, 1379–1392. [CrossRef]
64. Kamilia, S.; Thian, L.G.; Norbert, S.; Khai, E.L.; Eldawaty, M.; Rodeano, R. Debris flow susceptibility analysis using a bivariate statistical analysis in the Panataran River, Kg Melangkap, Sabah, Malaysia. *IOP Conf. Ser. Earth Environ. Sci.* **2022**, *1103*, 12038.
65. Lay, U.S.; Pradhan, B.; Yusoff, Z.B.M.; Abdallah, A.F.B.; Aryal, J.; Park, H.-J. Data Mining and Statistical Approaches in Debris-Flow Susceptibility Modelling Using Airborne LiDAR Data. *Sensors* **2019**, *19*, 3451. [CrossRef] [PubMed]
66. Han, L.; Zhang, J.; Zhang, Y.; Lang, Q. Applying a Series and Parallel Model and a Bayesian Networks Model to Produce Disaster Chain Susceptibility Maps in the Changbai Mountain area, China. *Water* **2019**, *11*, 2144. [CrossRef]
67. Chen, J.; Qin, S.; Li, G.; Peng, S.; Ma, Q.; Cao, C.; Liu, X.; Zhai, J. Debris Flow Susceptibility Assessment Based on RS-IVM Method in Jilin Province. *J. Basic Sci. Enginee Ring* **2021**, *29*, 1359–1371.
68. Federico, V.; Jayne, K.L.; Alain, C.; Marina, P.; Giandomenico, F. Investigation and numerical simulation of debris flow events in Rochefort basin (Aosta Valley—NW Italian Alps) combining detailed geomorphological analyses and modern technologies. *Bull. Eng. Geol. Environ.* **2022**, *81*, 378.
69. Hiroshi, T.; Masaharu, F.; Koichiro, O. Numerical modeling of debris flows using basic equations in generalized curvilinear coordinate system and its application to debris flows in Kinryu River Basin in Saga City, Japan. *J. Hydrol.* **2022**, *615*, 128636.
70. Fallas Salazar, S.; Rojas González, A.M. Evaluation of Debris Flows for Flood Plain Estimation in a Small Ungauged Tropical Watershed for Hurricane Otto. *Hydrology* **2021**, *8*, 122. [CrossRef]
71. Iylia, R.M.; Faizah, C.R.; Azahari, R.K.; Sumiaty, A.; Albati, K.S.; Aznah, N.A.; Aminaton, M.; Tetsuo, T.; Yusuke, O. Modelling Debris Flow Runout: A Case Study on the Mesilau Watershed, Kundasang, Sabah. *Water* **2021**, *13*, 2667.

72. Hou, S.; Cao, P.; Li, A.; Chen, L.; Feng, Z.; Liu, J.; Wang, L. Debris flow hazard assessment of the Eryang River watershed based on numerical simulation. *IOP Conf. Ser. Earth Environ. Sci.* **2021**, *861*, 62002. [CrossRef]
73. Zhang, W.; Chen, J.-P.; Wang, Q.; An, Y.; Qian, X.; Xiang, L.; He, L. Susceptibility analysis of large-scale debris flows based on combination weighting and extension methods. *Nat. Hazards* **2013**, *66*, 1073–1100. [CrossRef]
74. Zhong, D.; Xie, H.; Wei, F. Research on the regionalization of debris flow danger degree in the upper reaches of Changjiang river. *Mt. Res.* **1994**, *12*, 65–70.
75. Liu, l.; Wang, S. Preliminary research of two-level fuzzy comprehensive evaluation on landslide and debris flow risk degree of a district. *J. Nat. Disasters* **1996**, *5*, 51–59.
76. Paudel, B.; Fall, M.; Daneshfar, B. GIS-based assessment of debris flow hazards in Kulekhani Watershed, Nepal. *Nat. Hazards* **2020**, *101*, 143–172. [CrossRef]
77. Ekawati, J.; Hardiman, G.; Pandelaki, E.E. Analysis of GIS-Based Disaster Risk and Land Use Changes in The Impacted Area of Mudflow Disaster Lapindo. *IOP Conf. Ser. Earth Environ. Sci.* **2020**, *409*, 12032. [CrossRef]
78. Kain, C.L.; Rigby, E.H.; Mazengarb, C. A combined morphometric, sedimentary, GIS and modelling analysis of flooding and debris flow hazard on a composite alluvial fan, Caveside, Tasmania. *Sediment. Geol.* **2018**, *364*, 286–301. [CrossRef]
79. Aronica, G.T.; Biondi, G.; Brigandì, G.; Cascone, E.; Lanza, S.; Randazzo, G. Assessment and mapping of debris-flow risk in a small catchment in eastern Sicily through integrated numerical simulations and GIS. *Phys. Chem. Earth Parts A/B/C* **2012**, *49*, 52–63. [CrossRef]